PHYSICAL REVIEW B VOLUME 22, NUMBER 6 15 SEPTEMBER 1980

Network dynamics

M. F. Thorpe
Physics Department, Michigan State University, East Lansing, Michigan 48824

F. L. Galeener
Xerox Palo Alto Research Center, Palo Alto, California 94304

(Received 25 February 1980; revised manuscript received 4 August 1980)

A Lagrangian formalism is set up within which the vibrational spectrum of any covalently bonded network with nearest-neighbor central forces can be discussed. The covalent bonds are used as directions that define coordinate axes at each site. The nonorthogonality and in some cases overcompleteness of the displacements is taken care of in a simple way within the Lagrangian formulation. It is shown that the vibrational eigenvalues can be obtained from the corresponding quantities for the connectivity matrix of the network. This allows the spectral limits delineating the allowed spectral regions to be found, and their dependence on the masses and bond angles is simply exposed.

I. INTRODUCTION

While there is a substantial amount of experimental data[1] on the vibrational properties of glasses from infrared absorption and Raman scattering, the theory is in a much less well-developed state. The lack of microscopic translational invariance prevents the vibrational excitations being described by plane waves propagating from unit cell to unit cell. The principal theoretical approaches used to date have involved either numerical techniques to determine the modes of the random network[2,3] or attempts to identify molecular fragments that retain their integrity to some degree in the amorphous solid.[4]

An alternative approach was introduced recently by Sen and Thorpe.[5] This involves treating *only* the nearest-neighbor central forces in the network and neglecting other forces such as the angle-bending forces[6] and the long-range Coulomb effects.[7] These other forces are often much smaller and there is mounting evidence that most of the essential qualitative physics is contained in the nearest-neighbor central forces. Sen and Thorpe used the position of two delta functions to interpret the high-frequency modes of AX_2 glasses (BeF_2, GeS_2, $GeSe_2$, SiO_2, and GeO_2), and considerable insight into the vibrational spectra was obtained. In particular, the spectra of BeF_2 GeS_2, and $GeSe_2$ are dominated by molecular effects whereas solid-state effects are most important in SiO_2 and GeO_2.

Subsequently, Galeener[8] has shown that the central-force model of Sen and Thorpe[5] gives results within 5% of those obtained by the large cluster calculations of Bell, Dean, and Hibbins-Butler,[9] which include both central and noncentral forces. Galeener[8] also showed that band-edge motions derived from the central force model are able to explain the large highly polarized Raman line seen in tetrahedral SiO_2, GeO_2, and BeF_2 glasses. This first explanation of the origin of the dominant Raman line in tetrahedral glasses has been discussed mathematically by Martin and Galeener[10] and it has been suggested that the central force model also explains the primary Raman and ir modes seen in vitreous As_2O_3, As_2S_3, and As_2Se_3.[11] These quantitative and qualitative successes of the Sen and Thorpe model for tetrahedral glasses have encouraged us to carry out the present work.[12]

In this paper we put the theory of Sen and Thorpe on a more complete and general theoretical basis using a Lagrangian formulation.[13] This allows extensions to be made to any network and we derive results for a number of glass structures. We believe that this approach will be very useful in interpreting experimental results without having to do large numerical calculations. Considerable insight is also obtained into the interplay between the structure and the vibrational properties of a glassy network. For example, changes in the spectrum due to structural changes caused by pressure or neutron irradiation can be readily understood.

The outline of this paper is as follows. In the next section we set up a general Lagrangian formalism for arbitrary networks. It is shown how the kinetic energy and potential energy can be written in terms of generalized coordinates for various local geometries and bonding schemes. In Sec. III, a number of specific networks are discussed in detail, and it is shown how the connectivity matrix of the network plays a vital role. Details of the connectivity matrix for various networks are given in the Appendix. An important goal of this work has been to provide sufficiently general results and detailed examples to enable

the reader to derive expressions for additional networks not considered herein. In the concluding section some brief comments are made about comparison with experimental results.

II. LAGRANGIAN FORMULATION OF NETWORK DYNAMICS

Restricting the problem to involve only nearest-neighbor central forces leads to great simplifications. The vibrational frequencies of the network ω can be expressed in terms of the eigenvalues of the connectivity matrix ϵ, discussed in the Appendix. Even if the detailed shape of the spectrum of eigenvalues $\rho(\epsilon)$ is not known, the spectral bounds on ϵ allow us to find spectral bounds for ω.

A. Potential energy

It is convenient to refer all displacements to *bond directions* rather than introduce an external coordinate system. The bond directions are described by unit vectors $\hat{q}$ and the amplitude of the displacement by q as shown in Fig. 1. For the network we use labels l, l', etc., to denote the *site* and Δ, Δ', etc., to denote the *bond* so the unit vectors are $\hat{q}_\Delta(l)$ and the amplitudes of the displacements are the generalized coordinates $q_\Delta(l)$. The displacements $q_\Delta(l)$, $q_{\Delta'}(l)$ are associated with the same *site*, whereas $q_\Delta(l), q_\Delta(l')$ are associated with the same *bond*. It is particularly simple to write down the potential energy V in this coordinate system:

$$V=\tfrac{1}{2}\alpha\sum_{\langle l,l',\Delta\rangle}[q_\Delta(l)+q_\Delta(l')]^2. \tag{2.1}$$

If there is more than one *type* of bond, then there will be more than one force constant α. The angular brackets below the summation mean that each bond is only counted once.

There are two disadvantages to using the $q_\Delta(l)$ rather than the three orthogonal components normally used in crystalline lattice dynamics:

(1) The $\hat{q}_\Delta(l)$ are not necessarily orthogonal, even at a single site l. This is not a serious complication and is easily handled within the Lagrangian formulation introduced below.

(2) In some cases the $\hat{q}_\Delta(l)$ form an overcomplete set. Only three are needed at each site to describe a vector displacement. If there are four or more bonds the set is overcomplete. If there are z bonds then we must introduce $(z-3)$ constraints at that site. This is most easily handled by including an additional term in the potential.

Neither of these disadvantages is sufficient enough to outweigh the tremendous advantages of not having to introduce the rotation matrices that relate an external coordinate system to the bond directions at each site in the disordered solid.

B. Kinetic energy

The kinetic energy T is a little more complicated to express in terms of the $q_\Delta(l)$ but we derive expressions below for the various site symmetries that will be encountered in this paper. We will consider the three cases that correspond to two-, three-, and four-coordinated atoms.

1. Two-coordinated atoms

A two-coordinated atom (such as O in SiO_2) is shown in Fig. 2, where the mass of the atom is m and the bond angle is θ. The transformation between the orthogonal unit vectors $\hat{x}$, $\hat{y}$ and the nonorthogonal unit vectors $\hat{q}_1$ and $\hat{q}_2$ that lie along the two bonds is

$$\begin{aligned}\hat{x}&=\tfrac{1}{2}(\hat{q}_1-\hat{q}_2)/\sin\tfrac{1}{2}\theta,\\ \hat{y}&=\tfrac{1}{2}(\hat{q}_1+\hat{q}_2)/\cos\tfrac{1}{2}\theta.\end{aligned} \tag{2.2}$$

If the atom is displaced from its equilibrium posi-

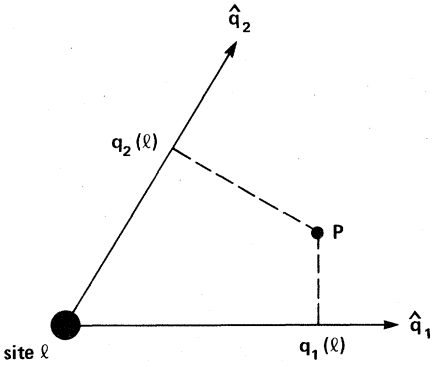

FIG. 1. Nonorthogonal two-dimensional coordinate system used to describe the displacement of a particle at site l to position P. The unit vectors $\hat{q}_1$ and $\hat{q}_2$ point along the bond directions and the displacement is characterized by amplitudes $q_1(l)$ and $q_2(l)$ in these directions.

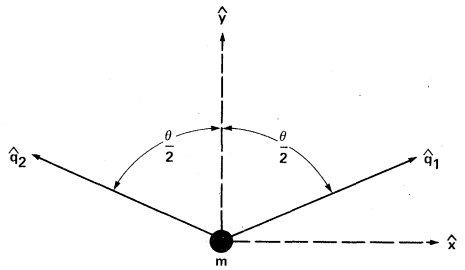

FIG. 2. Coordinate system used for a two-coordinated atom. The $\hat{y}$ axis bisects the angle between the two bonds denoted by $\hat{q}_1$ and $\hat{q}_2$, and the $\hat{x}$ axis is perpendicular to the $\hat{y}$ axis.

tion to P, then the displacement is $\vec{P}$ which may either be regarded as $\vec{P}(x,y)$ or $\vec{P}(q_1,q_2)$. These amplitudes transform in the same way as the unit vectors so that

$$x=\tfrac{1}{2}(q_1-q_2)/\sin\tfrac{1}{2}\theta\,,$$
$$y=\tfrac{1}{2}(q_1+q_2)/\cos\tfrac{1}{2}\theta\,. \tag{2.3}$$

The kinetic energy T can now be written as

$$T=\tfrac{1}{2}m(\dot{x}^2+\dot{y}^2+\dot{z}^2) \tag{2.4}$$
$$=\tfrac{1}{2}m[a(\dot{q}_1^2+\dot{q}_2^2)+\dot{q}_3^2+b(\dot{q}_1+\dot{q}_2)^2]\,, \tag{2.5}$$

where

$$a=(1-\cos\theta)^{-1}\,,$$
$$a+2b=(1+\cos\theta)^{-1}\,, \tag{2.6}$$

and the third generalized coordinate $q_3=z$. With nearest-neighbor central forces, the potential will be independent of q_3. This is usually referred to as a redundant coordinate, as it leads to a zero-frequency excitation. We shall omit it in the examples in this paper. The dot denotes time differentiation.

2. *Three-coordinated atoms*

A three-coordinated atom (such as As in As_2O_3) is shown in Fig. 3 where the mass of the atom is m and the angle between any two of the bonds is θ. The three vectors $\hat{q}_1$, $\hat{q}_2$, and $\hat{q}_3$ span the space. The $\hat{x},\hat{y},\hat{z}$ axes are set up as shown in Fig. 3 where the $\hat{x}$ axis is the projection of the $\hat{q}_1$ axis onto the plane perpendicular to $\hat{z}$. The angle made by $\hat{z}$ with either $\hat{q}_1$, $\hat{q}_2$, or $\hat{q}_3$ is α so that $3\sin^2\alpha = 4\sin^2\tfrac{1}{2}\theta$. The transformation equations are

$$\hat{q}_1=\hat{x}\sin\alpha-\hat{z}\cos\alpha\,,$$
$$\hat{q}_2=-\hat{x}\tfrac{1}{2}\sin\alpha+\hat{y}(\sqrt{3}/2)\sin\alpha-\hat{z}\cos\alpha\,, \tag{2.7}$$
$$\hat{q}_3=-\hat{x}\tfrac{1}{2}\sin\alpha-\hat{y}(\sqrt{3}/2)\sin\alpha-\hat{z}\cos\alpha\,.$$

The amplitudes transform in the same way as the unit vectors so that

$$q_1=x\sin\alpha-z\cos\alpha\,,$$
$$q_2=-x\tfrac{1}{2}\sin\alpha+y(\sqrt{3}/2)\sin\alpha-z\cos\alpha\,, \tag{2.8}$$
$$q_3=-x\tfrac{1}{2}\sin\alpha-y(\sqrt{3}/2)\sin\alpha-z\cos\alpha\,.$$

The kinetic energy is given by (2.4). Inverting (2.8), this kinetic energy becomes

$$T=\tfrac{1}{2}m[a'(\dot{q}_1^2+\dot{q}_2^2+\dot{q}_3^2)+b'(\dot{q}_1+\dot{q}_2+\dot{q}_3)^2]\,, \tag{2.9}$$

where

$$a'=(1-\cos\theta)^{-1}\,,$$
$$a'+3b'=(1+2\cos\theta)^{-1}\,. \tag{2.10}$$

A special case occurs when $\theta=120°$ and the three bonds become coplanar. In this case $a'=\frac{2}{3}$ and b' is irrelevant and can be set equal to zero, as there is the constraint

$$q_1+q_2+q_3=0 \tag{2.11}$$

that must be built into the Lagrangian. To get a complete form for the kinetic energy, (2.4) in this case, a fourth coordinate axis $\hat{q}_4$ must be introduced that is perpendicular to the plane defined by $\hat{q}_1$, $\hat{q}_2$, and $\hat{q}_3$. This gives an additional contribution to T which is $\frac{1}{2}m\dot{q}_4^2$.

3. *Four-coordinated atoms*

A four-coordinated atom (such as Si in SiO_2) is shown in Fig. 4 where the mass is m and the four bonds are assumed to be perfectly tetrahedral. The kinetic energy (2.4) can be expressed in terms of q_1, q_2, and q_3, only using the result for *three*-coordinated atoms with $\theta=\cos^{-1}(-\frac{1}{3})$, i.e.,

$$T=\tfrac{1}{2}m[\tfrac{3}{4}(\dot{q}_1^2+\dot{q}_2^2+\dot{q}_3^2)+\tfrac{3}{4}(\dot{q}_1+\dot{q}_2+\dot{q}_3)^2]\,. \tag{2.12}$$

Introducing the fourth coordinate axis $\hat{q}_4$, this can

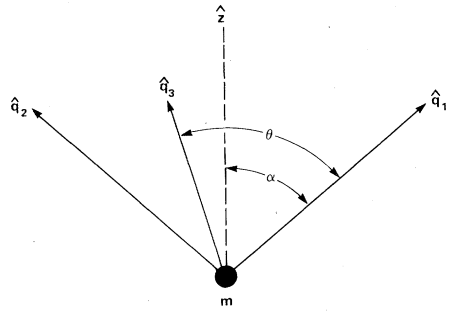

FIG. 3. Coordinate system used for a three-coordinated atom. The $\hat{z}$ axis is symmetrically positioned with respect to $\hat{q}_1$, $\hat{q}_2$, and $\hat{q}_3$. The $\hat{x}$ is the projection of the $\hat{q}_1$ axis onto the plane perpendicular to $\hat{z}$, and $\hat{y}$ completes the right-handed set $\hat{x}$, $\hat{y}$, $\hat{z}$.

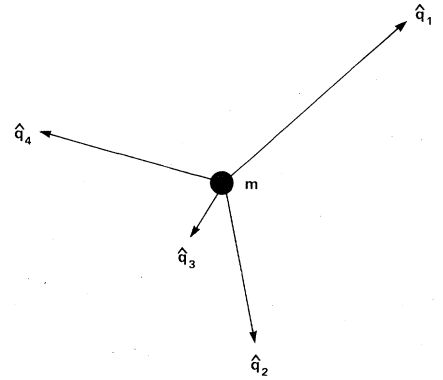

FIG. 4. Coordinate system used for a four-coordinated atom, where the four bonds $\hat{q}_1$, $\hat{q}_2$, $\hat{q}_3$, and $\hat{q}_4$ form a perfect tetrahedron.

be rewritten as

$$T=\tfrac{3}{8}m(\dot{q}_1^2+\dot{q}_2^2+\dot{q}_3^2+\dot{q}_4^2)\,, \tag{2.13}$$

with the constraint

$$q_1+q_2+q_3+q_4=0 \tag{2.14}$$

that must be built into the Lagrangian. These three cases cover all the forms for the kinetic energy that we will need in this paper.

C. Equations of motion

The complete Lagrangian L is defined by[13]

$$L(\{q_i,\dot{q}_i\})=T(\{\dot{q}_i\})-V(\{q_i\})\,, \tag{2.15}$$

where the curly brackets $\{\cdots\}$ denote the whole set of q_i, $\dot{q}_i$, etc., over all i. The equations of motion are

$$\frac{d}{dt}\left(\frac{\partial L}{\partial\dot{q}_i}\right)-\frac{\partial L}{\partial q_i}=0\,, \tag{2.16}$$

where q_i, $\dot{q}_i$ are regarded as independent variables. This generates a set of linear equations for the network whose solution for particular networks is discussed in the following sections.

If the set of q_i is overcomplete, account must be taken of the linear constraints [e.g., see Eqs. (2.11) and (2.14)] in constructing the Lagrangian or the equations of motion. The most convenient and physical way is to add a term to the potential which for the constraints (2.11) and (2.14) would look like

$$V\to V+\tfrac{1}{2}\lambda\sum_l\left(\sum_\Delta q_\Delta(l)\right)^2. \tag{2.17}$$

For finite λ, there are extra degrees of freedom. However, as $\lambda\to\infty$, some of the frequencies become infinite, and the remaining finite frequencies are consistent with the constraints

$$\sum_\Delta q_\Delta(l)=0 \quad \text{for all } l\,. \tag{2.18}$$

We have found the Lagrangian formulation of network dynamics to be both necessary and easy to use, as demonstrated in the next section for various networks.

D. Mode counting

Because our model contains only nearest-neighbor central forces, there are some zero-frequency modes. These arise because the network can be distorted in such a way that *all the bond lengths are unchanged*. There is no restoring force associated with this kind of motion. If the network has N_s sites, there are $3N_s$ degrees of freedom. The sites need not be equivalent and can have different numbers of nearest-neighbor bonds. Keeping a single bond length fixed is one constraint. If the network has N_b bonds, where a bond is defined by having two sites connected by a central force, then there are N_b independent constraints and the following are true:

(i) The number of zero-frequency modes $=3N_s-N_b$,
(ii) The number of finite-frequency modes $=N_b$. (2.19)

Of course (2.19) is only applicable if $3N_s>N_b$. This is always the case in the covalent networks considered in this paper. It would not be so in an elemental network where each atom has *more than six nearest neighbors* connected by central forces. In this case there would be no zero-frequency modes (except of course for the three acoustic modes that correspond to rigid lateral displacements). Equation (2.19) is an important result and provides a useful check that one has found all the finite-frequency modes whose total should be N_b.

Another useful check on the work in this paper is sometimes provided by a knowledge of the trace of the dynamical matrix. For a system with central forces (not necessarily nearest neighbors), α_{ij} connecting sites i and j with mass M_i, M_j, it can easily be shown that

$$\sum_l\omega_l^2=\sum_{i,j}\frac{\alpha_{ij}}{M_i}\,. \tag{2.20}$$

This trace is just the sum of the frequencies of isolated diatomic molecules with masses M_i and M_j at either end of springs α_{ij}.

III. APPLICATION TO SPECIFIC NETWORKS

In this section we apply the general ideas described in Sec. II to particular types of networks.

A. Silicon networks

Amorphous Si (or Ge) is perhaps the simplest and best studied continuous random network. Each atom is assumed to be perfectly tetrahedrally coordinated as shown in Fig. 4. From Eqs. (2.1), (2.13), (2.14), and (2.17) the Lagrangian L may be written as

$$L=\tfrac{3}{8}M\sum_{l,\Delta}[\dot{q}_\Delta(l)]^2-\tfrac{1}{2}\alpha\sum_{\langle l,l',\Delta\rangle}[q_\Delta(l)+q_\Delta(l')]^2 -\tfrac{1}{2}\lambda\sum_l\left(\sum_\Delta q_\Delta(l)\right)^2, \tag{3.1}$$

where λ is a Lagrange multiplier that will tend to infinity eventually. This takes care of the constraint at each site l:

$$\sum_\Delta q_\Delta(l)=0\,. \tag{3.2}$$

The equation of motion (2.16) for $q_\Delta(l)$ is

$$\tfrac{3}{4}M\ddot{q}_\Delta(l)+\alpha[q_\Delta(l)+q_\Delta(l')]+\lambda\sum_\Delta q_\Delta(l)=0\,, \quad (3.3a)$$

where it is implied in (3.3) that l' is a nearest neighbor of l associated with the same bond Δ. We look for normal modes where $q_\Delta(l)$ has a time dependence $\exp(i\omega t)$ so that (3.3a) becomes

$$(\alpha-\tfrac{3}{4}M\omega^2)q_\Delta(l)+\alpha q_\Delta(l')+\lambda Q(l)=0\,, \quad (3.3b)$$

where

$$Q(l)=\sum_\Delta q_\Delta(l) \quad (3.4)$$

is the "s"-like part of the displacement. The $Q(l)$ becomes zero as $\lambda\to\infty$.

A similar equation to (3.3b) can be written for $q_\Delta(l')$, which is then eliminated between the two equations to give

$$(\alpha-\tfrac{3}{4}M\omega^2)q_\Delta(l)-\alpha^2 q_\Delta(l)+\lambda(\alpha-\tfrac{3}{4}M\omega^2)Q(l) = \lambda\alpha Q(l')\,. \quad (3.5)$$

Summing over all l' (which is one of the four neighbors of l) we have an equation involving only $Q(l)$:

$$(\alpha-\tfrac{3}{4}M\omega^2)Q(l)-\alpha^2 Q(l)+4\lambda(\alpha-\tfrac{3}{4}M\omega^2)Q(l) = \lambda\alpha\sum_{l'}Q(l')\,. \quad (3.6)$$

This can be rewritten as

$$\sum_{l'}Q(l')=\epsilon Q(l)\,, \quad (3.7)$$

with

$$\epsilon=(1/\lambda\alpha)[(\alpha-\tfrac{3}{4}M\omega^2)^2+4\lambda(\alpha-\tfrac{3}{4}M\omega^2)-\alpha^2]\,. \quad (3.8)$$

Equation (3.7) will be recognized as just the eigenvalue equation for the connectivity matrix (A2b) discussed in the Appendix. Consequently, a knowledge of the eigenvalues of the connectivity matrix ϵ leads to the eigenfrequencies of the vibrational problem via Eq. (3.8). Finally we let $\lambda\to\infty$ and drive off to infinite frequency the unwanted modes associated with the extra degrees of freedom and from (3.8) we find

$$M\omega^2=\tfrac{1}{3}\alpha(4-\epsilon)\,, \quad (3.9)$$

a result previously found by Weaire and Alben.[14] Using (A3b), we see that $0\le\omega^2\le 8\alpha/3M$.

The connectivity matrix has 1 state per site. If the Si network has N sites, then (3.9) leads to N eigenfrequencies ω^2. However the general result (2.19) shows that there should be $2N$ finite frequencies. The other modes do not have an "s"-like component, even for finite λ. They are not contained within Eq. (3.6) but are included in (3.3b). Putting ω^2 equal to its maximum value in (3.9) $(8\alpha/3M)$ Eq. (3.3b) becomes

$$\alpha q_\Delta(l)=\alpha q_\Delta(l')+\lambda Q(l)\,. \quad (3.3c)$$

This can be satisfied if $q_\Delta(l)-q_\Delta(l')=0$ for every bond Δ (remembering that l, l' are sites at either end of the bond Δ). There is thus one independent choice of $q_\Delta(l)$ for each bond or $2N$ in all. However to satisfy (3.3c) we must ensure that $Q(l)=0$ for every site l. This leads to N constraints so that there are $2N-N=N$ modes at $\omega^2=8\alpha/3M$. Similarly, there are N modes at $\omega^2=0$, where (3.3b) becomes

$$-\alpha q_\Delta(l)=\alpha q_\Delta(l')+\lambda Q(l) \quad (3.3d)$$

and we put $q_\Delta(l)+q_\Delta(l')=0$ for each bond Δ. This is in accord with the general result (2.19) and thus we have found all the modes. The modes at $\omega^2=0$ may be regarded as transverse acoustic and those at $\omega^2=8\alpha/3M$ as transverse optic, although this nomenclature only has real meaning in a crystalline solid.

The density of vibrational states in Ge is discussed with the aid of Fig. 5. Panel (a) is for nearest-neighbor central forces only,[14] while (b) also includes nearest-neighbor noncentral forces,[15] which broaden the delta functions in (a). Panel (c) again shows the central plus noncentral force result, replotted for comparison with the experimentally determined density of states[16] of crystalline Ge, given in panel (d). Comparison of panels (a) and (d) shows that the central-force model predicts the main features in the density of states (i.e., the four main peaks). Comparison of panels (a) and (b) reveals that the transverse acoustic and optic peaks in (b) have their origin in the delta functions of (a). Delta functions appear in the density of states for all networks when only nearest-neighbor central forces are included.

B. GaAs networks

The results of Sec. III A can be rather easily generalized to an AB network like GaAs where every A-type atom is surrounded by four B-type atoms and every B-type atom is surrounded by four A-type atoms. This means that the network must contain only even rings or nearest-neighbor bonds. Such networks have been constructed and studied.[17]

The Lagrangian is identical to (3.1) except that the mass M is replaced by M_A or M_B, as appropriate. This carries through to Eq. (3.3b) where M is replaced by M_A or M_B depending on whether l is an A- or B-type site, respectively:

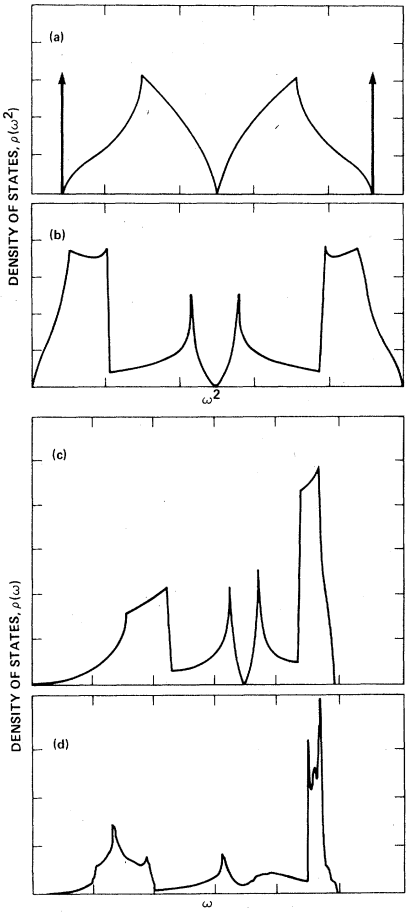

FIG. 5. Density of vibrational states for Ge. The horizontal scales for (a) and (b) are frequency *squared*, while those for (c) and (d) are linear in frequency ω. Panel (a) is for a central force model (Ref. 14) [see Eq. (3.9) in the text], while (b) also includes nearest-neighbor noncentral forces (Ref. 15). It can be seen that the delta functions become the TA and TO peaks and the two peaks in the band in (a) are squeezed together to become the LA and LO peaks. (c) is the same as (b) but plotted against ω, and (d) is the experimentally determined vibrational density of states for crystalline Ge (Ref. 16).

$$(\alpha - \tfrac{3}{4}M_A\omega^2)q_\Delta(l) + \alpha q_\Delta(l') + \lambda Q(l) = 0\,,$$
$$(\alpha - \tfrac{3}{4}M_B\omega^2)q_\Delta(l) + \alpha q_\Delta(l') + \lambda Q(l) = 0\,. \qquad (3.3e)$$

Equation (3.6) for an A site becomes

$$(\alpha - \tfrac{3}{4}M_A\omega^2)(\alpha - \tfrac{3}{4}M_B\omega^2)Q(l) - \alpha^2 Q(l) + 4\lambda(\alpha - \tfrac{3}{4}M_B\omega^2)Q(l) = \lambda\alpha\sum_{l'} Q(l') \qquad (3.10)$$

and a similar equation at a B site. As $\lambda \to \infty$ these equations correspond to (A6) with

$$\epsilon_A = (3M_B\omega^2 - 4\alpha)\alpha^{-1}\,,$$
$$\epsilon_B = (3M_A\omega^2 - 4\alpha)\alpha^{-1}\,, \qquad (3.11)$$
$$\epsilon' = 0\,,$$

so that Eq. (A7a) (which relates to the eigenvalues of the connectivity matrix) becomes

$$(3M_A\omega^2 - 4\alpha)(3M_B\omega^2 - 4\alpha) = \epsilon^2\alpha^2\,, \qquad (3.12)$$

i.e.,

$$\omega^2 = \frac{2\alpha}{3}\left(\frac{1}{M_A} + \frac{1}{M_B}\right) \pm \left\{\left[\frac{2\alpha}{3}\left(\frac{1}{M_A} - \frac{1}{M_B}\right)\right]^2 + \frac{\alpha^2\epsilon^2}{9M_AM_B}\right\}^{1/2}. \qquad (3.13)$$

This is the required generalization of (3.9) when M_A and M_B are not equal. With $z_A = z_B = 4$, we have from (A4a) that $0 < \epsilon^2 < 16$. The outer band edges (corresponding to $\epsilon^2 = 16$) also have delta functions with weight N (where there are $\frac{1}{2}N$ AB units in the network) associated with them and occur at

$$\omega^2 = 0 \quad \text{and} \quad \tfrac{4}{3}\alpha(1/M_A + 1/M_B)\,. \qquad (3.14)$$

The inner band edges, caused by the mass difference, occur at

$$\omega^2 = 4\alpha/3M_A \quad \text{and} \quad 4\alpha/3M_B\,. \qquad (3.15)$$

There are no delta functions associated with the inner band edges. Comparison with the Si result shows that the mass difference splits the band into two bands each with weight $\frac{1}{2}N$. This has been discussed previously by Thorpe[18] for a more general force constant model.

C. ABX_4 networks

An interesting generalization of the AB tetrahedral network is obtained by inserting a 2-connected X atom between each AB pair, producing what is here referred to as an ABX_4 network. We treat the special case where all X–A–X and X–B–X angles are tetrahedral and all A–X–B angles have the common value θ. This network is pictured schematically in Fig. 6. (Note that the X–B distance does not necessarily equal the X–A distance.) To our knowledge, no glass has been shown to have this structure, but there are several for which it may be an appropriate idealized model, including $SiGeO_4$, $GaAsO_4$, and other amorphous III-V oxides. In the special case $A = B$, this network corresponds to the tetrahedral 4-2 glasses such as SiO_2, GeO_2, BeF_2, etc.

To simplify notation, we use the $q_\Delta(l)$ for the A and B atoms but $x_\Delta(l)$ for the X atoms. Using the results of Sec. II for two- and four-coordinated atoms, the Lagrangian for the whole system is

$$L=\tfrac{3}{8}\sum_{l,\Delta}M_l[\dot{q}_\Delta(l)]^2+\tfrac{1}{2}m\sum_l\left[a\sum_\Delta[\dot{x}_\Delta(l)]^2+b\Big(\sum_\Delta\dot{x}_\Delta(l)\Big)^2\right]-\tfrac{1}{2}\sum_{\langle l,l',\Delta\rangle}\alpha_l[q_\Delta(l)+x_\Delta(l')]^2-\tfrac{1}{2}\lambda\sum_l\Big(\sum_\Delta q_\Delta(l)\Big)^2, \tag{3.16}$$

where $M_l=M_A$ or M_B and $\alpha_l=\alpha_A$ or α_B as appropriate. The λ term is introduced as in Sec. III A because the $q_\Delta(l)$ form an overcomplete set at each site. The coefficients a and b are given by (2.6). The equations of motion for $q_\Delta(l)$ and $x_\Delta(l')$ are

$$\tfrac{3}{4}M_l\ddot{q}_A(l)+\alpha_l[q_\Delta(l)+x_\Delta(l')]+\lambda\sum_\Delta q_\Delta(l)=0 \tag{3.17}$$

and

$$m\Big(a\ddot{x}_\Delta(l')+b\sum_{\Delta'}\ddot{x}_{\Delta'}(l')\Big)+\alpha_l[x_\Delta(l')+q_\Delta(l)]=0\,. \tag{3.18}$$

Putting in the $\exp(i\omega t)$ time dependence of the $q_\Delta(l)$ and $x_\Delta(l)$ and eliminating the $x_\Delta(l)$ from Eqs. (3.17) and (3.18), we obtain

$$(\alpha_l^d-\tfrac{3}{4}M_l\omega^2)q_\Delta(l)+\alpha' q_\Delta(l')+\lambda Q(l)=0\,, \tag{3.19}$$

where

$$\alpha'=-m\omega^2\alpha_A\alpha_B\cos\theta\times[(m\omega^2)^2-(\alpha_A+\alpha_B)m\omega^2+\alpha_A\alpha_B\sin^2\theta]^{-1} \tag{3.20}$$

and

$$\alpha_l^d=\alpha_l+\frac{\alpha_l[\alpha_l m\omega^2-\alpha_A\alpha_B\sin^2\theta]}{[(m\omega^2)^2-(\alpha_A+\alpha_B)m\omega^2+\alpha_A\alpha_B\sin^2\theta]}\,, \tag{3.21}$$

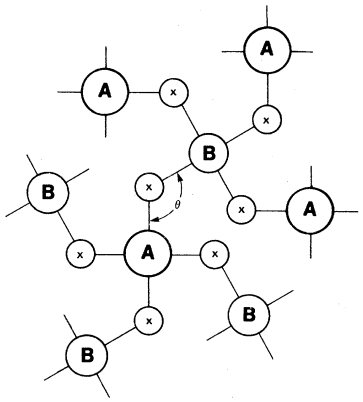

FIG. 6. Schematic drawing showing a piece of an ABX_4 network. The A and B atoms are tetrahedrally coordinated, and all the A–X–B bond angles are θ.

and $l=A$ or B as appropriate. The Eqs. (3.19) through (3.21) are very similar in structure to Eq. (3.3e) except that a single force constant α appears in (3.3e), whereas three frequency-dependent force constants appear in (3.19). This leads to a simple generalization of Eqs. (3.11) to give

$$\epsilon_A=(3M_B\omega^2-4\alpha_B^d)(\alpha')^{-1}\,,$$
$$\epsilon_B=(3M_A\omega^2-4\alpha_A^d)(\alpha')^{-1}\,, \tag{3.22}$$
$$\epsilon'=0\,.$$

Equation (A7a), which relates to the eigenvalues of the connectivity matrix, becomes

$$(3M_A\omega^2-4\alpha_A^d)(3M_B\omega^2-4d_B^d)=(\alpha'\epsilon)^2\,. \tag{3.23}$$

Putting in the explicit frequency dependence of α_A^d, α_B^d, and α [Eqs. (3.20) and (3.21)], this leads to a fourth-order polynomial for ω^2,

$$\mathfrak{A}\mathfrak{B}=(m\alpha_A\alpha_B\epsilon\cos\theta)^2\,,$$

where

$$\mathfrak{A}=4m\alpha_A(m\omega^2-\alpha_B)-3M_A[(m\omega^2)^2-(\alpha_A+\alpha_B)m\omega^2+\alpha_A\alpha_B\sin^2\theta]\,,$$
$$\mathfrak{B}=4m\alpha_B(m\omega^2-\alpha_B)-3M_B[(m\omega^2)^2-(\alpha_A+\alpha_B)m\omega^2+\alpha_A\alpha_B\sin^2\theta]\,, \tag{3.24}$$

which allows the vibrational frequencies ω^2 to be determined from the eigenvalues ϵ of the connectivity matrix. Every value of ϵ^2 leads to four frequencies ω, or (a better way of looking at it) every value of ϵ leads to two values of ω. Because the structure of ABX_4 has only even rings of bonds in the skeleton AB network, the eigenvalue spectrum of the connectivity matrix is symmetric about $\epsilon=0$, and for every eigenvalue $+\epsilon$ there is a corresponding one $-\epsilon$. In effect we have eliminated the twofold bonds and related the eigenfrequencies of the ABX_4 network to those of the connectivity matrix of the skeleton AB network. This can always be done with atoms that are twofold coordinated. It cannot be done for higher coordination numbers.

The quartic equation (3.24) must be solved numerically in general. However, simple expressions can be obtained for the frequencies of the band edges. Noting that $0<\epsilon^2<16$, we put $\epsilon^2=16$ in (3.24) to obtain

$$(\omega_1^\pm)^2=\frac{\alpha_A+\alpha_B}{2m}\pm\left[\left(\frac{\alpha_A-\alpha_B}{2m}\right)^2+\frac{\alpha_A\alpha_B\cos^2\theta}{m^2}\right]^{1/2} \tag{3.25}$$

and

$$(\omega_2^{\pm})^2 = \frac{\alpha_A+\alpha_B}{2m} + \frac{2}{3}\left(\frac{\alpha_A}{M_A}+\frac{\alpha_B}{M_B}\right) \pm \left\{\left[\frac{\alpha_A-\alpha_B}{2m}+\frac{2}{3}\left(\frac{\alpha_A}{M_A}-\frac{\alpha_B}{M_B}\right)\right]^2+\frac{\alpha_A\alpha_B\cos^2\theta}{m^2}\right\}^{1/2}. \tag{3.26}$$

By using arguments similar to those used for Si it can be shown that there are delta functions with weight N at $\omega_2^{\pm}$ (where there are $2N$ ABX_4 units in the network). The other four band edges, caused by the difference between the A and B atoms, occur when $\epsilon^2 = 0$ and are given by

$$(\omega_3^{\pm})^2 = \frac{\alpha_A+\alpha_B}{2m} + \frac{2}{3}\frac{\alpha_A}{M_A} \pm \left[\left(\frac{\alpha_A-\alpha_B}{2m}+\frac{2\alpha_A}{3M_A}\right)^2+\frac{\alpha_A\alpha_B\cos^2\theta}{m^2}\right]^{1/2}, \tag{3.27}$$

$$(\omega_4^{\pm})^2 = \frac{\alpha_A+\alpha_B}{2m} + \frac{2}{3}\frac{\alpha_B}{M_B} \pm \left[\left(\frac{\alpha_A-\alpha_B}{2m}-\frac{2\alpha_B}{3M_B}\right)^2+\frac{\alpha_A\alpha_B\cos^2\theta}{m^2}\right]^{1/2}. \tag{3.28}$$

These band edges are shown in Fig. 7(c) for the *hypothetical* case of $GeSiO_4$. In this figure, $\alpha(\text{Ge–O}) = 431$ N/m and $\alpha(\text{Si–O}) = 545$ N/m, values deduced from a central force analysis of data on GeO_2 and SiO_2 glasses, respectively.[8] The band edges for the latter AX_2 tetrahedral glasses are shown in Figs. 7(a) and 7(b).

For the special case when $M = M_A = M_B$ and $\alpha = \alpha_A = \alpha_B$, Eqs. (3.25) through (3.28) reduce to

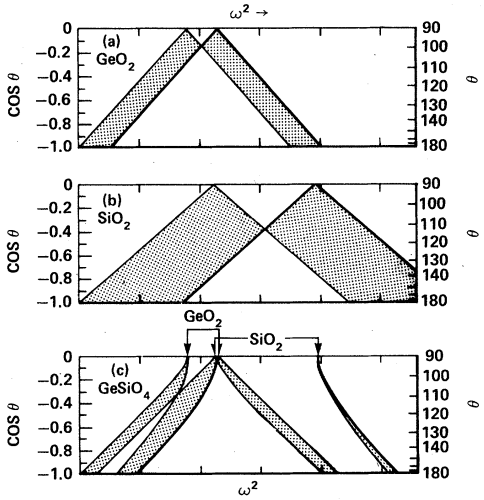

FIG. 7. The allowed frequency bands for GeO_2, SiO_2, and $GeSiO_4$ as discussed in the text. The band edges shown by heavier lines have delta functions associated with them as discussed in the text.

those for AX_2 glasses derived by Sen and Thorpe[5] (where there is an extensive discussion of the behavior of the modes as a function of θ). Figure 7(c) shows that extra splittings appear in the ABX_4 bands due to the A, B mass difference. Also as $\theta = 90°$, the network decouples into the molecular modes of AX_4 tetrahedra at

$$\omega^2 = \frac{\alpha_A}{m} \text{ and } \frac{\alpha_A}{m}+\frac{4\alpha_A}{3M_A} \tag{3.29}$$

and molecular modes of the BX_4 tetrahedra at

$$\omega^2 = \frac{\alpha_B}{m} \text{ and } \frac{\alpha_B}{m}+\frac{4\alpha_B}{3M_B}. \tag{3.30}$$

In each case, the first mode is the high-frequency singlet and the second mode the high-frequency triplet of the tetrahedral molecule as discussed in Sen and Thorpe. There is weight $\frac{1}{2}N$ in each of the four bands to give a total weight of $4N$ including the delta functions. The other $5N$ modes are at zero frequency.

The bands for $GeSiO_4$ are perhaps surprisingly narrow when compared to GeO_2 and SiO_2 in Fig. 7. This is because it is difficult for the modes centered on one Ge to hybridize with those centered on another, the intervening Si having modes at quite different frequencies. A similar argument holds for modes primarily associated with the Si atoms. This "shielding" effect is particularly apparent in the very narrow band at the highest frequencies in Fig. 7(c). This effect will be less pronounced if the Ge and Si atoms take up random (rather than alternating) positions in the network. Nevertheless, at sufficiently low concentrations of Si substituted into a GeO_2 network, the highest-frequency band should be very narrow as would be expected for a local mode.

D. A_3B_4 (Ge_3As_4) networks

In Sec. III A we worked with tetrahedrally four-coordinated atoms, such as Si, and in Sec. III C we added two-coordinated atoms, such as O. In the present section we introduce trigonally three-coordinated atoms, typified, e.g., by As. In particular we treat an idealized A_3B_4 network in which each A atom is tetrahedrally coordinated to four B atoms, while each B atom is trigonally coordinated to three A atoms. This local order is depicted schematically in Fig. 8, where all A–X–A angles have the same value θ. In general, $0° \leq \theta \leq 120°$. We alternatively call this the Ge_3As_4 network, since it *may* provide an idealized model for a glassy form of Ge_3As_4.

For notation, we use $q_\Delta(l)$ for the A atoms (Ge) and $x_\Delta(l)$ for the B atoms (As). Using the results of Sec. II for three- and four-coordinated atoms, the Lagrangian for the whole system is

$$L=\tfrac{3}{8}M\sum_{l,\Delta}[\dot{q}_\Delta(l)]^2+\tfrac{1}{2}m\sum_{l}\left[a'\sum_{\Delta}[\dot{x}_\Delta(l)]^2+b'\left(\sum_{\Delta}\dot{x}_\Delta(l)\right)^2\right]-\tfrac{1}{2}\alpha\sum_{\langle l,l',\Delta\rangle}[q_\Delta(l)+x_\Delta(l')]^2$$
$$-\tfrac{1}{2}\lambda\sum_{l}\left(\sum_{\Delta}q_\Delta(l)\right)^2, \tag{3.31}$$

where M is the mass of the A atom and m the mass of the B atom. The λ term is introduced, as in Sec. IIIA, because the $q_\Delta(l)$ form an overcomplete set at each site. The coefficients a' and b' are given by (2.10).

The equations of motion for the $q_\Delta(l)$ and $x_\Delta(l')$ are

$$\tfrac{3}{4}M\ddot{q}_\Delta(l)+\alpha[q_\Delta(l)+x_\Delta(l')]+\lambda\sum_{\Delta}q_\Delta(l)=0 \tag{3.32}$$

and

$$m\left(a'\ddot{x}_\Delta(l')+b'\sum_{\Delta'}x_{\Delta'}(l')\right)+\alpha[x_\Delta(l')+q_\Delta(l)]=0\,. \tag{3.33}$$

Putting in the $\exp(i\omega t)$ time dependence of the $q_\Delta(l)$ and $x_\Delta(l')$ and writing

$$X(l')=\sum_{\Delta}x_\Delta(l') \tag{3.34}$$

and

$$Q(l)=\sum_{\Delta}q_\Delta(l)\,, \tag{3.35}$$

we obtain

$$(\alpha-\tfrac{3}{4}M\omega^2)q_\Delta(l)+\alpha x_\Delta(l')+\lambda Q(l)=0\,, \tag{3.36}$$
$$(\alpha-ma'\omega^2)x_\Delta(l')+\alpha q_\Delta(l)-mb'\omega^2X(l')=0\,. \tag{3.37}$$

Eliminating $q_\Delta(l)$ from these two equations gives

$$(\alpha-\tfrac{3}{4}M\omega^2)(\alpha-ma'\omega^2)q_\Delta(l)-\alpha^2q_\Delta(l)$$
$$+\alpha mb'\omega^2X(l')+\lambda(\alpha-ma'\omega^2)Q(l)=0\,. \tag{3.38}$$

Summing over all Δ yields

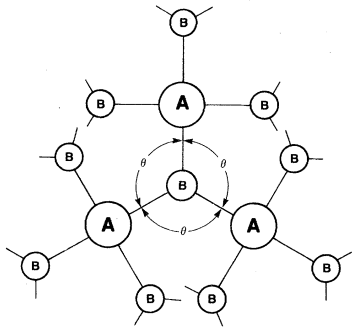

FIG. 8. Schematic diagram of an A_3B_4 network. Each A atom is tetrahedrally bonded and each B atom makes three bonds so that the A–B–A bond angles are all θ.

$$[(\alpha-\tfrac{3}{4}M\omega^2)(\alpha-ma'\omega^2)-\alpha^2]Q(l)+\alpha mb'\omega^2\sum_{l'}X(l')$$
$$+4\lambda(\alpha-ma'\omega^2)Q(l)=0 \tag{3.39}$$

and similarly eliminating $q_\Delta(l)$ from (3.36) and (3.37) gives

$$[(\alpha-\tfrac{3}{4}M\omega^2)(\alpha-ma'\omega^2)-\alpha^2]X(l')-\alpha\lambda\sum_{l}Q(l)$$
$$-3mb'\omega^2(\alpha-\tfrac{3}{4}M\omega^2)X(l')=0\,. \tag{3.40}$$

Those equations can be brought into correspondence with (A6) if we choose

$$\epsilon_A=[4\lambda(\alpha-ma'\omega^2)+(\alpha-ma'\omega^2)(\alpha-\tfrac{3}{4}M\omega^2)-\alpha^2]$$
$$\times(\alpha mb'\omega^2)^{-1}\,,$$
$$\epsilon_B=[3mb'\omega^2(\alpha-\tfrac{3}{4}M\omega^2)$$
$$-(\alpha-ma'\omega^2)(\alpha-\tfrac{3}{4}M\omega^2)-\alpha^2](\alpha\lambda)^{-1}\,, \tag{3.41}$$
$$\epsilon'=0.$$

Letting $\lambda\to\infty$, the eigenfrequencies ω^2 are related to the eigenvalues ϵ of the connectivity matrix by (A7a).

$$[4(\alpha-ma'\omega^2)]\{[\alpha-m(a'+3b')\omega^2](\alpha-\tfrac{3}{4}M\omega^2)-\alpha^2\}$$
$$+\alpha^2mb'\omega^2\epsilon^2=0\,, \tag{3.42}$$

which has the solution:

$$\omega^2=\frac{2\alpha}{3M}+\frac{(2+\cos\theta)\alpha}{2m}$$
$$\pm\left[\left(\frac{2\alpha}{3M}+\frac{3\alpha\cos\theta}{2m}\right)^2-\frac{\alpha^2\epsilon^2\cos^2\theta}{3Mm}\right]^{1/2}. \tag{3.43}$$

Thus for every root of the connectivity matrix, two eigenfrequencies are generated. The eigenvalue spectra is bounded by $0<\epsilon^2<12$, and so the band edges for ω^2 are obtained by putting $\epsilon^2=0$ and 12 to give

$$\omega_1^2=(\alpha/m)(1+2\cos\theta)\,,$$
$$\omega_2^2=(\alpha/m)(1-\cos\theta)\,,$$
$$\omega_3^2=\omega_1^2+4\alpha/3M\,, \tag{3.44}$$
$$\omega_4^2=\omega_2^2+4\alpha/3M\,.$$

These bands are shown in Fig. 9 for the special case $M=2m$. If there are N A atoms, then the two bands each have weight N. The delta function at ϵ_B with weight $N_B - N_A = \frac{1}{3}N$ described in the Appendix is at ω_3^2 in Fig. 9. The remaining $\frac{5}{3}N$ states are in a delta function at ω_4^2. This gives a total of $4N$ modes which is equal to the total number of bonds [see (2.19)].

At $\theta = 90°$, the system decouples into the singlet and triplet modes of isolated AB_4 molecules. As the apex angle at the B atom opens up, these modes spread out into bands which cross over at θ_c, given by

$$\cos\theta_c = -4m/9M . \tag{3.45}$$

For $M=2m$, $\theta_c = 103°$.

The trace of the dynamical matrix (2.20) for this network is

$$\sum_i \omega_i^2 = 4N\left(\frac{1}{m}+\frac{1}{M}\right) . \tag{3.46}$$

This agrees with the same trace worked out using the eigenvalues (3.43) (the square root that involves ϵ^2 cancels between pairs of modes) *and remembering to include the contributions from the two delta functions.*

E. A_2X_5 (P_2O_5) networks

At this point we introduce one-coordinated atoms, such as singly bonded F or doubly bonded O. In particular, we treat the case of P_2O_5, which has been shown to be a network in which each P atom is surrounded almost tetrahedrally by three bridging oxygen atoms and one double-bonded oxygen terminator.[19] This kind of network is shown schematically in Fig. 10, where every bridging atom has the same A–X–A angle θ. Although not shown in the figure, we require the three single bonded X–A–X angles about each A atom to have the same value ψ. This network is especially useful to treat since it has numerous special cases corresponding to ideal structures for glasses other than P_2O_5.

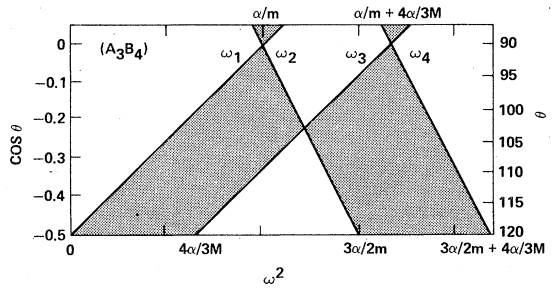

FIG. 9. Allowed frequency bands for an A_3B_4 network with mass ratio $M(A)=2m(B)$. The frequencies that define the band edges ω_1, ω_2, ω_3, ω_4 are given by (3.44). The band edges shown by heavier lines at ω_3 and ω_4 have delta functions associated with them as discussed in the text.

For notation, we use $q_\Delta(l)$ for the P atoms, $x_\Delta(l)$ for the singly bonded O atoms, and $y(l)$ refers to the P site to which the O is bonded. Using the results of Sec. IIB we only use *three* $q_\Delta(l)$ at each P atom. The fourth coordinate $q_4(l)$ is given in terms of the other three by

$$q_4(l) = c\sum_{\Delta=1}^{3} q_\Delta(l) , \tag{3.47}$$

where

$$c^2 = [3(1+2\cos\psi)]^{-1} . \tag{3.48}$$

Using the results of Sec. II for two- and three-coordinated atoms, the Lagrangian for the whole system is

$$L = \tfrac{1}{2}M\sum_l\left[a'\sum_\Delta[\dot q_\Delta(l)]^2 + b'\left(\sum_\Delta \dot q_\Delta(l)\right)^2\right] + \tfrac{1}{2}m\sum_{l'}\left[a\sum_\Delta[\dot x_\Delta(l')]^2 + b\left(\sum_\Delta \dot x_\Delta(l')\right)^2\right]$$
$$+\tfrac{1}{2}m'\sum_l[\dot y(l)]^2 - \tfrac{1}{2}\alpha\sum_{\langle l,l'\Delta\rangle}[q_\Delta(l)+x_\Delta(l')]^2 - \tfrac{1}{2}\beta\sum_l\left(c\sum_\Delta q_\Delta(l)+y(l)\right)^2 , \tag{3.49}$$

where M is the mass of the P and m is the mass of the O. It is convenient to use m' for the mass of the doubly bonded O even though we will put $m'=m$ at the end of the calculation. Here, α is the P—O single-bond force constant and β is the P=O double-bond force constant. The coefficients a, b are given by Eqs. (2.6) and a', b' by Eqs. (2.10) with θ replaced by ψ. The equations of motion are

$$M\left(a'\ddot q_\Delta(l) + b'\sum_{\Delta'}\ddot q_{\Delta'}(l)\right) + \alpha[q_\Delta(l)+x_\Delta(l')]$$
$$+\beta c\left(c\sum_{\Delta'} q_{\Delta'}(l)+y(l)\right) = 0 , \tag{3.50}$$

$$m'\ddot y(l) + \beta\left(y(l)+c\sum_{\Delta'} q_{\Delta'}(l)\right) = 0 , \tag{3.51}$$

$$m\left(a\ddot x_\Delta(l') + b\sum_{\Delta'}\ddot x_{\Delta'}(l')\right) + \alpha[x_\Delta(l')+q_\Delta(l)] = 0 . \tag{3.52}$$

Putting in the $\exp(i\omega t)$ time dependence of the $q_\Delta(l)$, $x_\Delta(l)$, and $y(l)$ and using (3.51) to eliminate the $y(l)$, we obtain

$$(\alpha - Ma'\omega^2)q_\Delta(l) + \alpha x_\Delta(l)$$
$$+\left(\frac{\beta c^2 m'\omega^2}{m'\omega^2-\beta} - Mb'\omega^2\right)Q(l) = 0 \tag{3.53}$$

and

$$(\alpha - ma\omega^2)x_{\triangle}(l') + \alpha q_{\triangle}(l) - mb\omega^2 X(l') = 0 \ . \tag{3.54}$$

These equations are very similar to (3.36) and (3.37). Proceeding as in that case, we can identify

$$\epsilon_A = \frac{3(\alpha - ma\omega^2)[\beta c^2 m'\omega^2/(m'\omega^2 - \beta) - Mb\omega^2] + (\alpha - ma\omega^2)(\alpha - Ma'\omega^2) - \alpha^2}{\alpha mb\omega^2} \ ,$$

$$\epsilon_B = \frac{2mb\omega^2(\alpha - Ma'\omega^2) - (\alpha - ma\omega^2)(\alpha - Ma'\omega^2) - \alpha^2}{\alpha[\beta c^2 m'\omega^2/(m'\omega^2 - \beta) - Mb'\omega^2]} \ , \tag{3.55}$$

$$\epsilon' = 0 \ .$$

The eigenfrequencies ω^2 are related to the eigenvalues ϵ of the connectivity matrix of a network with $z_A = 3$ and $z_B = 2$ and can be found using (A7a) where $0 < \epsilon^2 < 6$. This is an alternative to the technique used in SiO_2 and ABX_4 networks where the coordinates of the twofold coordinated atom were eliminated. There is always this choice with two-coordinated atoms. The equation relating ω^2 to ϵ^2 becomes

$$\mathfrak{A}'\mathfrak{B}' + \alpha^2 mb[\beta c^2 m'/(m'\omega^2 - \beta) - Mb']\epsilon^2 = 0 \ ,$$

where

$$\begin{aligned} \mathfrak{A}' &= ma[M(a' + 3b') - 3\beta c^2 m'/(m'\omega^2 - \beta)]\omega^2 - \alpha[ma + M(a' + 3b')] - 3\beta c^2 m'/(m'\omega^2 - \beta) \ , \\ \mathfrak{B}' &= m(a + 2b)Ma'\omega^2 - \alpha[m(a + 2b) + Ma'] \ . \end{aligned} \tag{3.56}$$

This leads to a quartic equation for ω^2. We assume the P atom to be perfectly tetrahedrally coordinated so that $a = b = \frac{3}{4}$. The band edges are given by $\epsilon^2 = 0$ and $\epsilon^2 = 6$.

$$(\omega_{1,5})^2 = \frac{1}{2}\left(\alpha\left(\frac{1 + \cos\theta}{m} + \frac{1}{3M}\right) - \beta\left(\frac{1}{m'} + \frac{1}{M}\right) \pm \left\{\left[\alpha\left(\frac{1 + \cos\theta}{m} + \frac{1}{3M}\right) - \beta\left(\frac{1}{m'} + \frac{1}{M}\right)\right]^2 + \frac{4\alpha\beta}{3M^2}\right\}^{1/2}\right) \tag{3.57}$$

and

$$(\omega_{2,6})^2 = \frac{1}{2}\left(\alpha\left(\frac{1 - \cos\theta}{m} + \frac{1}{3M}\right) + \beta\left(\frac{1}{m'} + \frac{1}{M}\right) \pm \left\{\left[\alpha\left(\frac{1 - \cos\theta}{m} + \frac{1}{3M}\right) - \beta\left(\frac{1}{m'} + \frac{1}{M}\right)\right]^2 + \frac{4\alpha\beta}{3M^2}\right\}^{1/2}\right), \tag{3.58}$$

where ω_1 and ω_2 are associated with the positive square roots and ω_5 and ω_6 with the negative ones. Also we have the results

$$\omega_3^2 = \frac{\alpha}{m}(1 + \cos\theta) + \frac{4\alpha}{3M} \tag{3.59}$$

and

$$\omega_4^2 = \frac{\alpha}{m}(1 - \cos\theta) + \frac{4\alpha}{3M} \ . \tag{3.60}$$

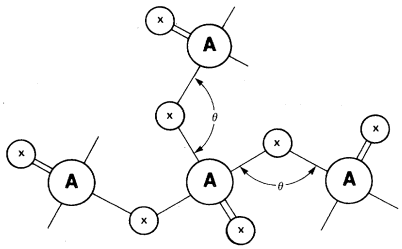

FIG. 10. Schematic diagram of an A_2X_5 network where the A–X–A bond angle is θ.

The bands are shown in Fig. 11, using parameters[19] approximately appropriate for P_2O_5: $\alpha = 450$ N/m, $\beta = 1160$ N/m. If there are N P atoms, then there is weight N in each of the three bands and weight $\frac{1}{2}N$ in each of the delta functions at ω_3 and ω_4. The diagram is very much like the others

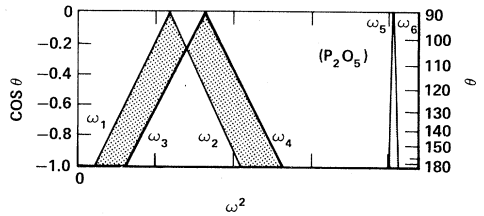

FIG. 11. Allowed frequency bands for P_2O_5 networks using the appropriate masses for P and O and a ratio of force constants for the O double and single bonds of 2.6. The six band-edge frequencies ω_i are given by Eqs. (3.57)–(3.60). The band edges shown by heavier lines at ω_3 and ω_4 have delta functions associated with them as discussed in the text.

obtained previously except for the narrow band at high frequencies associated with the stretching of the oxygen double bond.

F. A_2X_3 (As_2O_3) networks

The formula (3.56) is particularly interesting because it contains a number of other networks as special cases. Putting $\beta = 0$ yields an A_2X_3 network. Using θ for the A–X–A bond angle and ψ for the X–A–X bond angle as shown in Fig. 12, we find the eigenfrequencies are given by

$$\omega^2 = \frac{\alpha}{m} + \frac{(2+\cos\psi)\alpha}{2M} \pm \left[\left(\frac{3\alpha\cos\psi}{2M}\right)^2 + \left(\frac{\alpha\cos\theta}{m}\right)^2 - \frac{\alpha^2\cos\theta\cos\psi\epsilon}{mM}\right]^{1/2}, \tag{3.61}$$

where ϵ are the eigenvalues of the connectivity matrix for the A *skeleton network* [as used in Eq. (3.24) and in Sen and Thorpe]. This leads to band edges at

$$\begin{aligned}
\omega_1^2 &= \frac{\alpha}{m}(1+\cos\theta) + \frac{\alpha}{M}(1+2\cos\psi),\\
\omega_2^2 &= \frac{\alpha}{m}(1-\cos\theta) + \frac{\alpha}{M}(1+2\cos\psi),\\
\omega_3^2 &= \frac{\alpha}{m}(1+\cos\theta) + \frac{\alpha}{M}(1-\cos\psi),\\
\omega_4^2 &= \frac{\alpha}{m}(1-\cos\theta) + \frac{\alpha}{M}(1-\cos\psi).
\end{aligned} \tag{3.62}$$

These are plotted in Fig. 13 using parameters[11,20] appropriate for As_2O_3: $\psi = 98°$, $\alpha = 297$ N/m. If there are N A atoms, then each of the two bands shown in Fig. 13 has weight N and there is weight $\frac{1}{2}N$ in each of the two delta functions at ω_3 and ω_4.

Another special case occurs when the angle $\psi = 120°$ and the three bonds from the A atom are planar. We will refer to this as the B_2O_3 network. In this case Eqs. (3.62) become

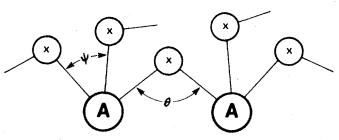

FIG. 12. Schematic diagram of an A_2X_3 network where θ is the A–X–A bond angle and ψ is the X–A–X bond angle.

$$\begin{aligned}
\omega_1^2 &= \frac{\alpha}{m}(1+\cos\theta),\\
\omega_2^2 &= \frac{\alpha}{m}(1-\cos\theta),\\
\omega_3^2 &= \frac{\alpha}{m}(1+\cos\theta) + \frac{3\alpha}{2M},\\
\omega_4^2 &= \frac{\alpha}{m}(1-\cos\theta) + \frac{3\alpha}{2M},
\end{aligned} \tag{3.63}$$

with the same weights as associated with (3.62).

G. As networks

Results for the As network may be derived from (3.62) by putting $\theta = 180°$, letting $m \to 0$, and also letting $\alpha \to 2\alpha'$, in order to have α' as the As–As force constant. Infinite solutions are rejected. The equivalent form of (3.61) is

$$\omega^2 = \frac{\alpha'}{M}[2 + (1+\epsilon)\cos\psi], \tag{3.64}$$

where $-3 \leq \epsilon \leq 3$. If there are N As atoms, then the band contains N states and there are $\frac{1}{2}N$ states associated with the delta function at

$$\omega_2^2 = \frac{2\alpha'}{M}(1-\cos\psi). \tag{3.65}$$

The other band edge is at

$$\omega_1^2 = \frac{2\alpha'}{M}(1+2\cos\psi). \tag{3.66}$$

These results are plotted in Fig. 14.

IV. DISCUSSION

We have set up a general Lagrangian formalism for examing network dynamics in the approximation of nearest-neighbor central forces. One of our results reproduces the expressions derived by Sen and Thorpe[5] for the band edges of AX_2 glasses. These expressions have been used else-

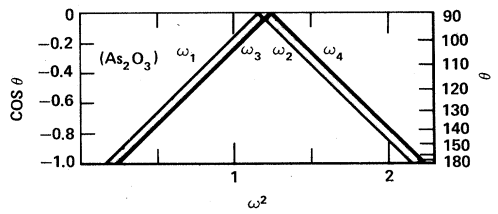

FIG. 13. Allowed frequency bands for an As_2O_3 network using appropriate masses for As and O and putting $\psi = 98°$. The four band-edge frequencies ω_i are given by Eqs. (3.62). The band edges shown by heavier lines at ω_3 and ω_4 have delta functions associated with them as discussed in the text.

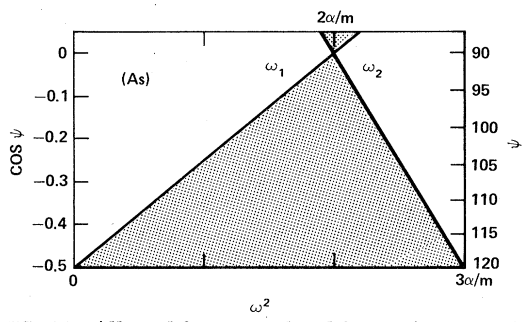

FIG. 14. Allowed frequency band for an As network where ψ is the As–As–As bond angle, m is the As mass, and α is the As–As force constant. The frequency ω_1 is given by Eq. (3.66). The frequency ω_2 is given by Eq. (3.65) and shown by the heavier line to indicate that there is a delta function associated with it.

where[8] for a detailed interpretation of the vibrational spectra of vitreous SiO_2, GeO_2, and BeF_2 with surprising success. Expressions were also obtained for the band edges of several other simple networks, including those appropriate for ABX_4 tetrahedral glasses, A_2X_5 and A_2X_3 trigonal glasses. The most important final formulas are Eqs. (3.25)–(3.28), Eqs. (3.44), and Eqs. (3.57)–(3.60); numerous idealized networks can be treated as special cases of these results. Detailed comparison of the new expressions with experimantal results on such glasses as P_2O_5 and As_2O_3 is planned and will be published elsewhere. Since the fundamental *physical* assumptions used in the present paper are the same as those used by Sen and Thorpe, it is expected that the new results will apply to the appropriate glasses with similar accuracy.

An important advantage of the central force model is that it yields *simple formulas* for the vibrational frequencies of a coupled network of atoms, thereby revealing directly the effect of changes in atomic mass, force constants, and bond angles. This information is much more difficult to obtain from large-cluster[2] or Bethe lattice[3] numerical calculations. Moreover, the simple formulas can be inverted to enable direct calculation of force constants and bond angles from a small number of observed frequencies, as has been done[8] for vitreous SiO_2, GeO_2, and BeF_2. For example, the densification of some glasses can be thought to take place by reduction of the bridging oxygen angle angle θ, without change in the force constant. Equations like (3.63) allow simple interpretation of the effect of such densification upon the vibrational frequencies. In this way Galeener[21] has interpreted the shifts of vibrational bands in neutron-irradiated GeO_2 as representing densification upon bombardment. Similar shifts should be seen upon application of hydrostatic pressure to glasses, and it would be interesting to contrast the behavior of glasses[22] like SiO_2 in which the tetrahedra are strongly coupled[5] with glasses like GeS_2 in which they are coupled less strongly.[5]

Isolated molecule models such as the one proposed by Lucovsky and Martin[4] also have the virtue of yielding simple formulas for vibrational frequencies. In these models the frequencies of vitreous SiO_2 (for example) are calculated from those of a hypothetical SiO_4 tetrahedral "molecule" and perhaps also from those of a Si–O–Si water-like "molecule." It has recently been demonstrated that such models are quantitatively and qualitatively inadequate,[23,24] except in those few cases where the structural units are weakly coupled. (Here, weak coupling means that $\theta \simeq 90°$ and noncentral forces are also weak, as is thought to be the case for GeS_2 glass.) The quantitative accuracy of the central-force model for vitreous SiO_2 GeO_2 and BeF_2 is due to the fact that the large values of θ (~140°) ensure that the two central forces acting noncollinearly on a bridging oxygen atom give rise to angle restoration tendencies much greater than those due to intrinsic angle restoring (*noncentral*) forces. Only *one* of the two noncollinear central forces on an oxygen atom is included in the isolated tetrahedal molecule model. The resultant error is greater than any improvement provided by the ability of the isolated molecule model to treat intrinsic noncentral forces.

The principal missing elements in the model developed in this paper are noncentral forces, Coulomb forces, and the treatment of matrix-element effects. The intrinsic noncentral forces mentioned in the preceding paragraph are typically about $\frac{1}{5}$ the magnitude of the nearest-neighbor central forces,[8] and their neglect is most important for the low-frequency modes.[8,25] It is possible that they can be included via perturbation theory. The long-range Coulomb forces may produce TO-LO splittings of the stronger infrared-active modes,[7] which are usually the higher-frequency modes. It is not known how to include these forces in the model at the present time. It has been shown quite generally that strong matrix-element effects can be expected in infrared and (especially Raman scattering experiments on glasses,[26] contrary to earlier predictions.[27] This has been demonstrated to be so in the case of vitreous SiO_2, GeO_2, and BeF_2, where the dominant Raman line is ascribed to a singular Raman matrix element occurring at the lowest-frequency band edge in the central force model.[8] A mathematical treatment has been developed using the central-force model and a bond polarizability Raman tensor.[10] We hope to make further progress in including

these effects, albeit at the expense of losing some of the extreme simplicity of the present model.

ACKNOWLEDGMENTS

We should like to thank R. J. Elliott, G. Lucovsky and R. M. Martin for useful discussions. M. F. T. would like to thank the Xerox Palo Alto Research Center for their hospitality during a summer visit. The work of M. F. T. was supported in part by NSF Grant No. DMR-77-05983. The work of F. L. G. is supported in part by the Office of Naval Research.

APPENDIX

In this appendix we discuss the *connectivity matrix* of a network, referred to frequently in the main text. This describes the *topological properties* of the network. It has been used frequently in the past in discussing the electronic band structure of amorphous solids.[28] In this paper we show how it can be used in vibrational spectra.

We consider a fully connected network where each site has nearest-neighbor bonds to z other sites. The connectivity matrix M is defined by its matrix elements,

$$M_{ij}=\begin{cases}1 & \text{if } i \text{ and } j \text{ are nearest neighbors,}\\ 0 & \text{otherwise.}\end{cases} \tag{A1}$$

This matrix is real and symmetric and the eigenvalues ϵ and eigenvectors $\vec{v}$ obey the equation

$$\underline{M}\,\vec{v}=\epsilon\vec{v}\ . \tag{A2a}$$

In the notiation used in the text, this equation would be written

$$\sum_{l'} Q(l')=\epsilon Q(l)\ . \tag{A2b}$$

Because the connectivity matrix is positive, we can apply the theorem of Frobenius[29] and taking $\vec{v}$ to be a positive vector all of whose elements are equal, we find that the eigenvalues ϵ are bounded by

$$|\epsilon|\leq z \tag{A3a}$$

or

$$-z\leq\epsilon\leq z\ . \tag{A3b}$$

This is the result that is used in establishing the spectral bounds in the main text.

A more complex network is formed when some of the sites A have z_A neighbors and some of the sites B have z_B neighbors. We suppose that all the neighbors of A are of type B and vice versa. The chemical formula for such a network would be $A_{z_B}B_{z_A}$. The connectivity matrix is again defined by (A1) but is more complex in that some rows have z_A nonzero entries, while others have z_B nonzero entries. The positive vector $\vec{v}$ may be taken to have equal entries v_A corresponding to all A sites and v_B corresponding to all B sites: Then $\vec{v}$ is an eigenvector if we choose $(v_A/v_B)^2=z_B/z_A$, and we find that the eigenvalues ϵ are bounded by

$$|\epsilon|\leq(z_Az_B)^{1/2} \tag{A4a}$$

or

$$-(z_Az_B)^{1/2}\leq\epsilon\leq(z_Az_B)^{1/2}\ . \tag{A4b}$$

A still more general connectivity matrix can be formed for this network if diagonal terms ϵ_A, ϵ_B are also included so that M is now defined by

$$M_{ii}=\begin{cases}\epsilon_A & \text{if } i \text{ is an } A \text{ site,}\\ \epsilon_B & \text{if } i \text{ is a } B \text{ site,}\end{cases}$$
$$M_{ij}=\begin{cases}1 & \text{if } i \text{ and } j \text{ are nearest neighbors,}\\ 0 & \text{otherwise.}\end{cases} \tag{A5}$$

The eigenvalue equation (A2) can be written

$$\epsilon_AQ(l)+\sum_{l'} Q(l')=\epsilon'Q(l)\ ,$$
$$\epsilon_BQ(l)+\sum_{l'} Q(l')=\epsilon'Q(l)\ . \tag{A6}$$

As before, every A site has z_A neighbors of type B and every B site has z_B neighbors of type A. A little manipulation of (A6) will show that the eigenvalues ϵ of the connectivity matrix with nonzero ϵ_A, ϵ_B are related to the eigenvalues ϵ [Eq. (A4a)], which corresponds to setting $\epsilon_A=\epsilon_B=0$ by

$$(\epsilon')^2-(\epsilon_A+\epsilon_B)\epsilon'+\epsilon_A\epsilon_B=\epsilon^2\ , \tag{A7a}$$

i.e.,

$$\epsilon'=\tfrac{1}{2}(\epsilon_A+\epsilon_B)\pm\{[\tfrac{1}{2}(\epsilon_A-\epsilon_B)]^2+\epsilon^2\}^{1/2} \tag{A7b}$$

and using the result (A4a) (viz. $0<\epsilon^2<z_Az_B$) we find the four band edges are

$$\epsilon'=\tfrac{1}{2}(\epsilon_A+\epsilon_B)\pm\{[\tfrac{1}{2}(\epsilon_A-\epsilon_B)]^2+z_Az_B\}^{1/2}\ ,$$
$$\epsilon'=\epsilon_A\ , \tag{A8}$$
$$\epsilon'=\epsilon_B\ .$$

This is the main result of this appendix and includes previous results as special cases. For example, (A3b) is obtained by setting $\epsilon_A=\epsilon_B=0$ and $z_A=z_B=z$.

In using these results in the text, it is convenient to set $\epsilon'=0$ and allow ϵ_A and ϵ_B to be frequency-dependent quantities. The equation that determines the eigenfrequencies (A7a) then is simply

$$\epsilon_A \epsilon_B = \epsilon^2 \ . \qquad \text{(A7c)}$$

If there are N_A atoms of type A and N_B atoms of type B, then the two bands with edges given by (A8) contain N_A and N_B states, respectively. This can easily be seen by allowing $\epsilon_A - \epsilon_B$ to be large when the bands become well separated and there are N_A states around ϵ_A and N_B states around ϵ_B. The general result follows from continuity as $\epsilon_A - \epsilon_B$ is decreased in value.

The spectrum contains a delta function at ϵ_B with weight $N_B - N_A$ if $N_B > N_A$. This state is constructed by allowing the amplitude of the wave function on all the A atoms to be zero leading to N_B possible states. However, in order for this to be an eigenstate the sum of the amplitudes of the wave function on all the B atoms surrounding a given A atom must be zero, leading to N_A independent constraints and hence $N_B - N_A$ states at ϵ_B. The rest of the spectrum is symmetric about $\frac{1}{2}(\epsilon_A + \epsilon_B)$, each of the two subbands containing N_A states.

[1]See, for example, G. Lucovsky, in *Amorphous and Liquid Semiconductors*, edited by J. Stuke and W. Brenig (Taylor and Francis, London, 1974), p. 1099.

[2]P. Dean, Rev. Mod. Phys. 44, 127 (1972); R. J. Bell, Rep. Prog. Phys. 35, 1315 (1972); in *Methods in Computational Physics*, edited by G. Gilat (Academic, New York, 1976), p. 215.

[3]R. B. Laughlin and J. D. Joannopoulos, Phys. Rev. B 16, 2942 (1977); 17, 2790 (1978).

[4]G. Lucovsky and R. M. Martin, J. Non-Cryst. Solids 8–10, 185 (1972).

[5]P. N. Sen and M. F. Thorpe, Phys. Rev. B 15, 4030 (1977).

[6]For a discussion of several potential force field models, see, e.g., J. R. Ferraro and J. S. Ziomek, *Introductory Group Theory* (Plenum, New York, 1969), p. 129.

[7]F. L. Galeener and G. Lucovsky, Phys. Rev. Lett. 37, 1474 (1976).

[8]F. L. Galeener, Phys. Rev. B 19, 4292 (1979); also Bull. Am. Phys. Soc. 23, 338 (1978); and Ref. 24.

[9]R. J. Bell, P. Dean, and D. C. Hibbins-Butler, J. Phys. C 3, 2111 (1970).

[10]R. M. Martin and F. L. Galeener, Bull. Am. Phys. Soc. 24, 495 (1979); and unpublished.

[11]F. L. Galeener, G. Lucovsky, and R. H. Geils, Phys. Rev. B 19, 4251 (1979).

[12]M. F. Thorpe and F. L. Galeener, Bull. Am. Phys. Soc. 24, 457 (1979).

[13]H. Goldstein, *Classical Mechanics* (Addison-Wesley, Cambridge, 1950), p. 14ff.

[14]D. Weaire and R. Alben, Phys. Rev. Lett. 29, 1505 (1972).

[15]M. F. Thorpe, Phys. Rev. B 8, 5352 (1973).

[16]G. Nilsson and G. Nelin, Phys. Rev. B 5, 3151 (1972).

[17]G. A. N. Connell and R. J. Temkin, Phys. Rev. B 9, 5323 (1974).

[18]M. F. Thorpe, J. Phys. C 7, 4037 (1974).

[19]F. L. Galeener and J. C. Mikkelsen, Jr., Solid State Commun. 30, 505 (1979).

[20]C. Sourisseua and R. Mercier, Spectrochim. Acta Part A 34, 173 (1978); A. Müller, B. N. Cyvin, S. J. Cyvin, S. Pohl, and B. Krebs, *ibid.* 32, 67 (1976).

[21]F. L. Galeener, J. Non-Cryst. Solids 40, 527 (1980).

[22]K. Chow, W. A. Phillips, and A. I. Bienenstock, in *Phase Transitions and Their Applications in Material Science*, edited by L. E. Cross (Pergamon, Oxford, 1973), p. 333.

[23]The application of group-theoretical rules to the isolated molecule model does not predict the observed second-order Raman and infrared spectra of several glasses: F. L. Galeener, in *Light Scattering in Solids*, edited by M. Balkanski, R. C. C. Leite, and S. P. S. Porto (Flammarion, Paris, 1976), p. 641; F. L. Galeener and G. Lucovsky, in *Structure and Properties of Non-Crystalline Semiconductors*, edited by B. T. Kolomiets (Nauka, Leningrad, 1976), p. 305.

[24]F. L. Galeener, in *Lattice Dynamics*, edited by M. Balkanski (Flammarion, Paris, 1978), p. 345.

[25]R. Kulas and M. F. Thorpe, in *Structure and Excitations of Amorphous Solids*, edited by G. Lucovsky and F. L. Galeener (AIP, New York, 1976), p. 251.

[26]F. L. Galeener and P. N. Sen, Phys. Rev. B 17, 1928 (1978).

[27]R. Shuker and R. W. Gammon, Phys. Rev. Lett. 25, 222 (1970).

[28]D. Weaire and M. F. Thorpe, in *Computational Methods for Large Molecules and Localized States in Solids*, edited by F. Herman, A. D. McLean, and R. K. Nesbet (Plenum, New York, 1972), p. 295.

[29]See, e.g., R. Bellman, *Introduction to Matrix Analysis* (McGraw-Hill, New York, 1960), p. 278.